LA-UR -91-887

LA-UR--91-887

DE91 009951

TITLE MICROSTRUCTURE OF EPITAXIAL $YBa_2Cu_3O_7$ THIN FILMS

AUTHOR(S) T E Mitchell

SUBMITTED TO To be published in "Ceramic Superconductors" by the American Ceramic Society" Second Interantional Congrress on Ceramic Science & Technology, Orlando, FL, Nov 12-15, 1990

DISCLAIMER

Los Alamos National Laboratory
Los Alamos, New Mexico 87545

MICROSTRUCTURE OF EPITAXIAL $YBa_2Cu_3O_7$ THIN FILMS

T. E, Mitchell, Center for Materials Science, Los Alamos National Laboratory, Los Alamos, NM 87545, USA

ABSTRACT

Thin epitaxial films of $YBa_2Cu_3O_7$ on single crystal substrates have been prepared in situ by laser ablation and by post situ annealing of evaporated films of Cu, Y and BaF_2. Substrates include (001) $SrTiO_3$, $LaGaO_3$, and $LaAlO_3$. For both in situ and post situ annealed films, epitaxial (001) grains of $YBa_2Cu_3O_7$ form near the substrate but (100) and (010) grains tend to nucleate for thicknesses greater than ~ 0.5μm. 90° grain boundaries are therefore common, as well as other defects such as small angle boundaries, dislocations and stacking faults. High resolution electron microscopy of the substrate/superconductor interface shows regions of perfect epitaxy, distorted areas, amorphous regions and areas of interdiffusion. The relationship of observed microstructure to critical current density is discussed.

INTRODUCTION

Epitaxial thin films of $YBa_2Cu_3O_7$ (hereafter referred to as Y123) have been successfully grown by a variety of deposition techniques on a number of different single crystal substrates. In many cases, critical currents in excess of 10^{10} A/m^2 (10^6 A/cm^2) at 77K have been achieved even in magnetic fields of 1T. This is superior even to single crystals and, of course, much better than the critical currents achieved in sintered polycrystalline material. Epitaxial thin films of Y123 are therefore distinguished not only by the absence of "bad" defects (high angle grain boundaries) but also by the presence of "good" defects not present in single crystals. The nature of the "good" defects is not clear, as discussed later.

Successful thin film techniques[1,2] include not only physical methods (e.g. electron beam evaporation, molecular beam epitaxy, sputtering, laser ablation, plasma spraying) but also chemical methods (e.g. chemical vapor deposition, spray pyrolysis, sol-gel). These techniques can also be divided into in situ and post situ types. For in situ techniques, deposition is performed directly at temperature giving an epitaxial film of the correct structure although an intermediate temperature anneal in oxygen is usually required to give the optimum oxygen stoichiometry. For post situ techniques, deposition is usually performed onto a substrate at ambient temperature; the film has to be subsequently annealed to crystallize the structure epitaxially on the substrate followed by an intermediate temperature anneal again. Post situ annealing is generally incompatible with device fabrication and can produce rough surfaces. In situ techniques have the additional advantage of having one less step in the process.

Substrates which have been used for growing thin film superconductors include the perovskites $SrTiO_3$, $LaGaO_3$ and $LaAlO_3$ and other oxides such as MgO, $MgAl_2O_4$ spinel and yttrium stabilized cubic zirconia[1]. Important factors include low reactivity with $YBa_2Cu_3O_7$, good lattice matching for epitaxial growth, similar thermal expansion coefficient and low dielectric constant. The perovskites have the best combination of properties, although the dielectric constant $SrTiO_3$ is rather high. In the present paper, the microstructure of Y123 grown on these perovskite single crystal substrates will be described for films grown by a post situ annealing technique and an in situ laser ablation technique. A selection of previous papers on thin film microstructures is given in References [3] to [16].

A plot of J_c vs. magnetic field for a typical laser ablated film of Y123 of thickness 0.5μm on a (001) $SrTiO_3$ substrate is shown in Fig. 1. Current densities in excess of 10^6 A/cm^2 are maintained out to fields ~ 4T parallel to the film although the current density drops off more rapidly if the field is perpendicular to the film. Such good performance was at one time only found in post situ annealed films and can now be achieved for films grown in situ.

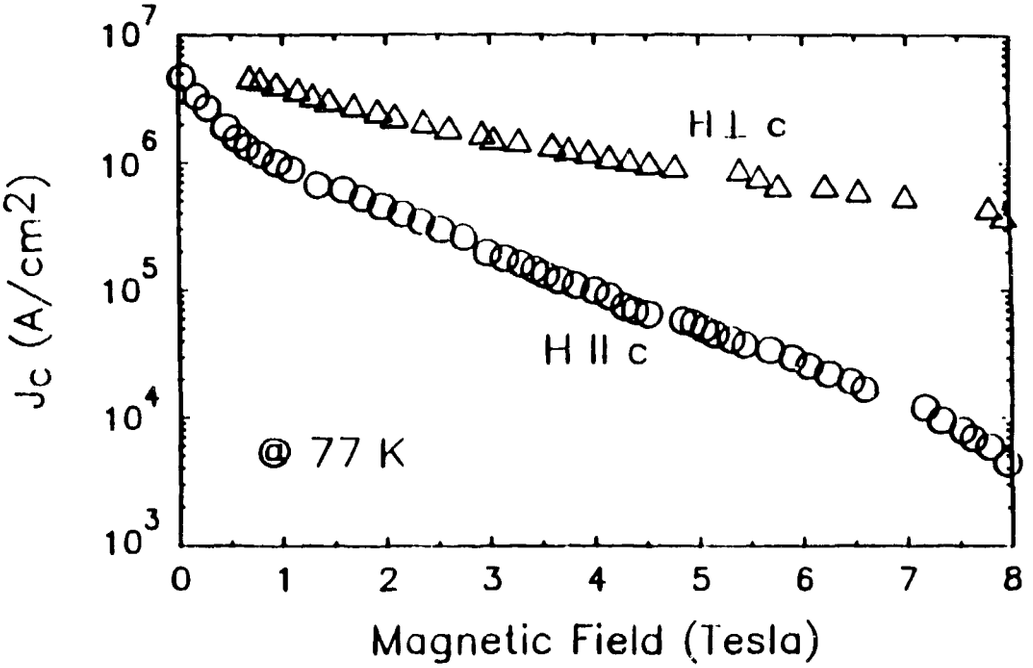

Figure 1. Typical J_c versus magnetic field plots for a Y123 film deposited by laser ablation onto (001) $LaAlO_3$ substrate.

THIN FILM DEPOSITION

Evaporated and annealed films were deposited by electron-beam evaporation of copper and yttrium and thermal evaporation of barium fluoride onto substrates at ambient temperature, a base pressure of 10^{-7} torr and a rate of 40Å/s[16]. The first post situ annealing step is in wet oxygen at about 850°C for 1h; the purpose of this step is to drive off the fluorine and partially oxidize the Y, Ba and Cu. The resulting amorphous film is then annealed in dry oxygen for 3h which further oxidizes and crystallizes the film; the crystallization apparently nucleates on the substrate since for suitable substrates (e.g. (001) $SrTiO_3$) the film is epitaxial. The film at this point is still tetragonal and further annealing in oxygen at 400°C is required to oxygenate fully to Y123 and transform to the superconducting orthorhombic form. Films with high T_c and J_c can be

grown up to 1μm in thickness. As described later, epitaxial crystallization of grains with the c-axis normal to the substrate occurs for thin films, i.e. the ab plane which carries the highest current lies in the plane of the film. For thicker films, grains with the c-axis parallel to the substrate tend to nucleate on the inner epitaxial grains, degrading the current carrying capacity. In addition, the c-axis parallel grains produce a basket weave pattern on the surface rather than a desirable smooth surface.

For laser deposited films a pulsed excimer laser was used (308 nm wavelength, 300 mJ, 30 ns pulses) with a beam area of 3 x 4 mm^2 onto a $YBa_2Cu_3O_7$ target in an oxygen pressure of 0.15 torr[17]. The substrate temperature is ~ 750°C and the deposition rate is around 150 Å/s. Epitaxial growth of tetragonal Y123 occurs directly (in situ growth). After deposition, the film is cooled to 400°C and annealed on oxygen (as with the evaporated films) in order to oxygenate and transform to the superconducting orthorhombic form. Again, the inner layers of Y123 grow with the c-axis normal to the substrate (for (001) $SrTiO_3$) but, for thicknesses greater than about 0.5 μm, the c-axis parallel grains tend to nucleate. An additional problem also occurs where particles of Y123 are ablated into the plasma and deposited directly onto the film with a random orientation. These and the c-axis parallel grains give a rough surface.

SUBSTRATES

As mentioned in the Introduction many substrates have been tried but the most successful have been the perovskites, $SrTiO_3$, $LaAlO_3$ and $LaGaO_3$, which closely match the lattice of Y123. Crystal data at ambient temperature are as follows:

$SrTiO_3$	Cubic Pm3m	a = 3.905Å
$LaAlO_3$	Rhombohedral R3m	a = 5.377Å, α = 60.13°
$LaGaO_3$	Orthorhombic Pbnm	a = 5.485, b = 5.521, c = 7.771Å
Y123	Orthorhombic Pmmm	a = 3.818, b = 3.884, c = 11.683Å

$SrTiO_3$ has the ideal perovskite structure while $LaAlO_3$ and $LaGaO_3$ have distorted structures which commonly occur in perovskite related compounds. Since the distortions are small, the structures can be described in terms of a smaller perovskite pseudo-cubic unit cell with parameters as follows:

$SrTiO_3$	3.905Å
$LaAlO_3$	3.792Å
$LaGaO_3$	3.891, 3.886Å
Y123	3.818, 3.884, 3.894Å

The close match between these numbers explains the epitaxy but it must be remembered that the epitaxy is established during deposition or annealing at high temperatures (750-850°C). The available data for the pseudo-cubic lattice constants as a function of temperature are shown in Fig. 2. The data for Y123 are for one atmosphere of oxygen; lower oxygen partial pressures give slightly higher lattice parameters and a lower tetragonal-to-orthorhombic transformation temperature[18]. The data for $SrTiO_3$ use the lattice parameter at 25°C and the known coefficient of thermal expansion. The data for $LaAlO_3$ and $LaGaO_3$ are from O'Bryan et al. [19]. $LaAlO_3$ gradually transforms from rhombohedral to cubic above about 400-500°C. $LaGaO_3$ transforms from orthorhombic to rhombohedral at 145°C. Since the epitaxy is established at high temperatures when Y123 is tetragonal, the parameters below are for 800°C and lattice mismatches are given for the a parameter of Y123 and the c/3 parameter.

	Parameter (Å)	Mismatch with a of Y123 (%)	Mismatch with c/3 of Y123 (%)
$SrTiO_3$	3.939	1.05	-1.24
$LaAlO_3$	3.834	-1.66	-3.94
$LaGaO_3$	3.923	0.64	-1.64
Y123: a	3.898	-	-2.28
Y123: c/3	3.988	2.28	-

This table shows that the a parameter has a better match than the c/3 parameter for all the substrates and thus explains the (001) epitaxy of Y123 with (001) substrates. The match is best for $LaGaO_3$, followed by $SrTiO_3$ and then $LaAlO_3$. However, it should be remembered that both $LaGaO_3$ and $LaAlO_3$ transform on cooling and that Y123 itself transforms during oxygenation. As seen in Fig. 2, the largest distortions are due to the transformation of Y123.

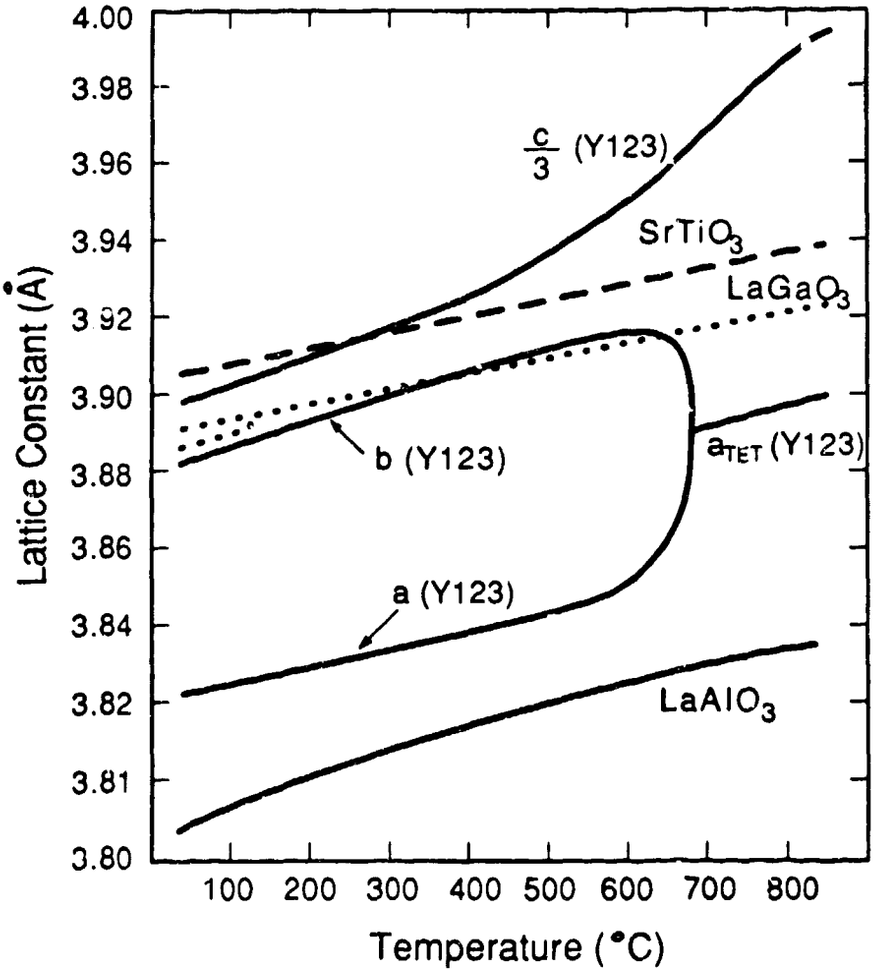

Figure 2. Plot of the pseudo-cubic lattice parameters of Y123, $SrTiO_3$, $LaGaO_3$ and $LaAlO_3$ versus temperature [18,19].

ELECTRON MICROSCOPY

Cross sectional specimens through the film and substrate were performed by the standard sandwich technique. Final thinning was done on a Gatan ion miller using liquid nitrogen cooling to minimize ion damage. Transmission electron microscopy (TEM) was performed on a Phillips CM30ST operating at 300kV. For high resolution electron microscopy (HREM), the point-to-point resolution was ~ 1.9Å. The specimen surface was also examined by scanning electron microscopy (SEM) using a Camscan instrument.

Evaporated and annealed films

Films prepared by evaporation and subsequent annealing in wet and dry oxygen have been grown on (001) substrates of both $SrTiO_3$ and $LaGaO_3$. A low magnification cross-sectional TEM micrograph of a Y123 films grown on $SrTiO_3$ is shown in Fig. 3. This is from an early poor quality film but it illustrates very well the important features in the microstructure. The total film thickness is 1.5 μm. There is an layer ~ 150 nm where the c-axis of the Y123 is normal to the substrate with perfect epitaxy. Beyond this inner layer most of the grains have their c-axis parallel to the substrate, either along [100] or [010]. They have a width of ~ 150 nm but they are elongated in the ab plane perpendicular to the substrate. Clearly with such a morphology the superconducting current is carried along the ab planes of the inner layer while the current carrying capacity of the outer grains is limited because they are wrongly oriented and because of the many 90° grain boundaries. Improved techniques have led to inner layers of ~ 0.5 μm thickness but growth of thicker layers has proved elusive.

Once the c-parallel grains nucleate, they grow rapidly in their ab planes to produce a rough surface. Fig. 4 shows SEM images of the surface of films of two thicknesses. Initially the films are smooth but, beyond the critical thickness, the surface becomes increasingly textured to a "basketweave" pattern[16]. This is because the two orientations of plate-shaped grains become increasingly dominant with the (001) planes of the plates being parallel to the (100) and (010) planes of the underlying substrate and the inner Y123 layer.

The perfect epitaxy of the inner Y123 layer with the $SrTiO_3$ layer can be seen in the HREM image in Fig. 5. The interface appears to be atomically perfect; even misfit dislocations are hard to find which is not surprising since the misfit at temperature is about 1% (Fig. 2). A 1% misfit would be completely accommodated by a dislocation every 100 atomic distances. There is also no evidence for interdiffusion or second phase formation at the interface. It is important that the substrate surface should be smooth before deposition. Large surface steps have been found to nucleate undesirable c-parallel grains.[11]

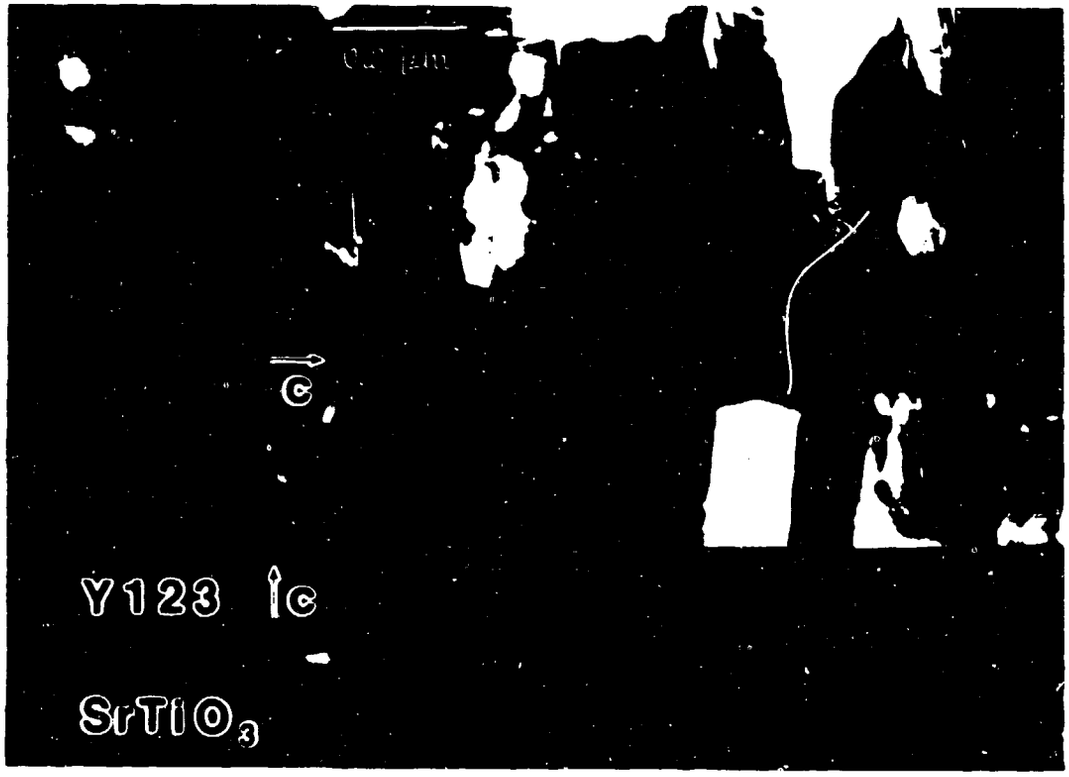

Figure 3. Low magnification TEM bright field image of a cross section through a Y123 film grown on (001) $SrTiO_3$. Note the transition from c-perpendicular to c-parallel grains.

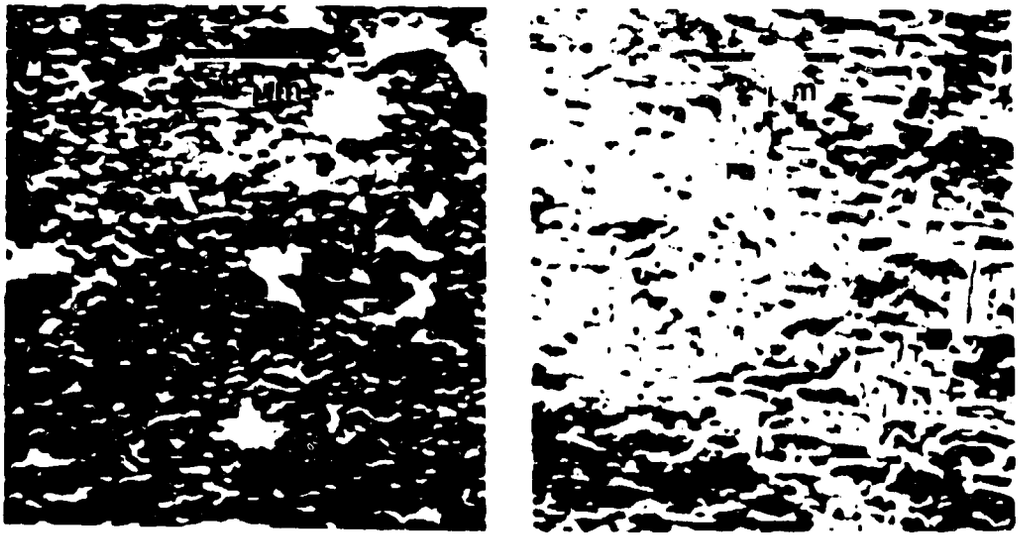

Figure 4. SEM images of Y123 film 0.26μm thick (left) and 0.56μm thick (right) on $SrTiO_3$.

Y123 grains have been grown on (001) $LaGaO_3$ substrates by the same technique. (Here (001) refers to the pseudo-cubic perovskite unit cell.) Values of J_c above $10^6 A/cm^2$ have been achieved at 77K with this substrate as well. Again there is a limit of about 0.5 μm for the growth of c-perpendicular grains. Examples of HREM images of the interface are shown in Fig. 6. These are viewed in the [110] direction rather than [100] for the $SrTiO_3$ substrate. Even so, there are notable differences in the $LaGaO_3$ case: (a) distorted regions, even where there are no interface dislocations, (b) amorphous regions and (c) regions showing evidence of interdiffusion. The distorted regions may be due to the phase transformations that occur in $LaGaO_3$ and Y123 with decreasing temperature. The rarity of interface dislocations is due to the small mismatch (0.5%) at the annealing temperature (Fig. 2). The amorphous regions are presumably due to local deviations from stoichiometry. Epitaxy is preserved because rapid growth of neighboring nuclei in the ab plane occurs such as to overlay the residual amorphous regions. The interdiffusion is not too surprising since La and Y can substitute for each other in Y123 and $LaGaO_3$ respectively; this must happen during the 850°C anneal. Interdiffusion occurs only over a few atomic distances and has little apparent effect on superconducting properties.

The Y123 epitaxial films are full of imperfections. The most common defects are the 90° grain boundaries that occur when the c-parallel grains nucleate on top of the c-perpendicular inner layer (Fig. 3). The grain boundaries parallel to the interface on top of the inner layer contain the (001) plane of the c-perpendicular grains and the (100) or (010) plane of the c-parallel grains. The grain boundaries of the elongated grains in the second layer are basically the same: (001) planes of one grain abut (100) or (010) planes of an adjacent grain. A HREM image of a typical 90° grain boundary is shown in Fig. 7. It is noteworthy that the a or b dimensions of one grain attempt to match the c/3 dimensions of the neighboring grain, leading to a periodic array of misfit dislocations in the boundary.

The most common defects within the grains are stacking faults and their associated partial dislocations. The faults are mostly extra Cu-O planes parallel to the interface, such as shown in Fig. 8. Accommodation of the extra Cu-O layer is accompanied by a shear of half a unit cell along the a or b axis[20]. The faults therefore terminate at partial dislocations with a Burgers vector of 1/6[031] or 1/6[301]. These faults presumably are due

Figure 5. HREM image of interface between Y123 and $SrTiO_3$ viewed along [100].

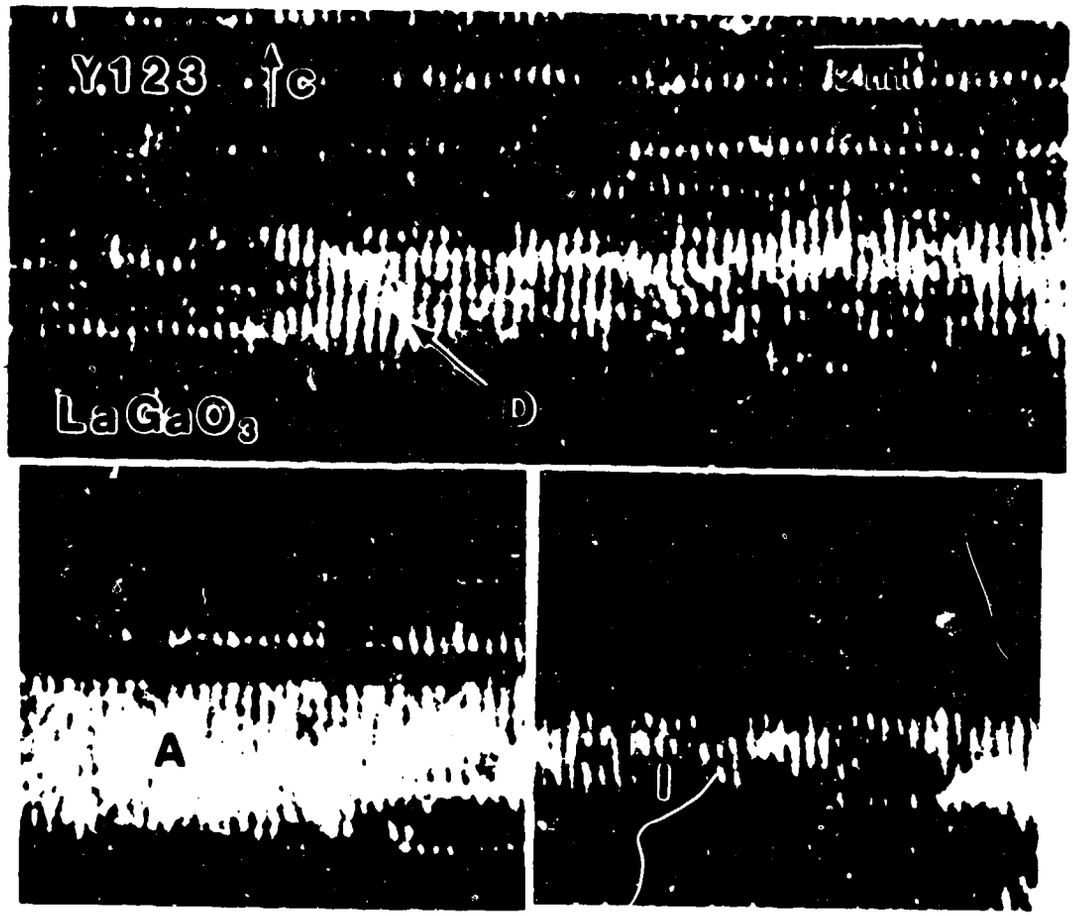

Figure 6. HREM images of Y123/$LaGaO_3$ viewed along [110] showing distorted (D), amorphous (A) and interdiffused regions (I).

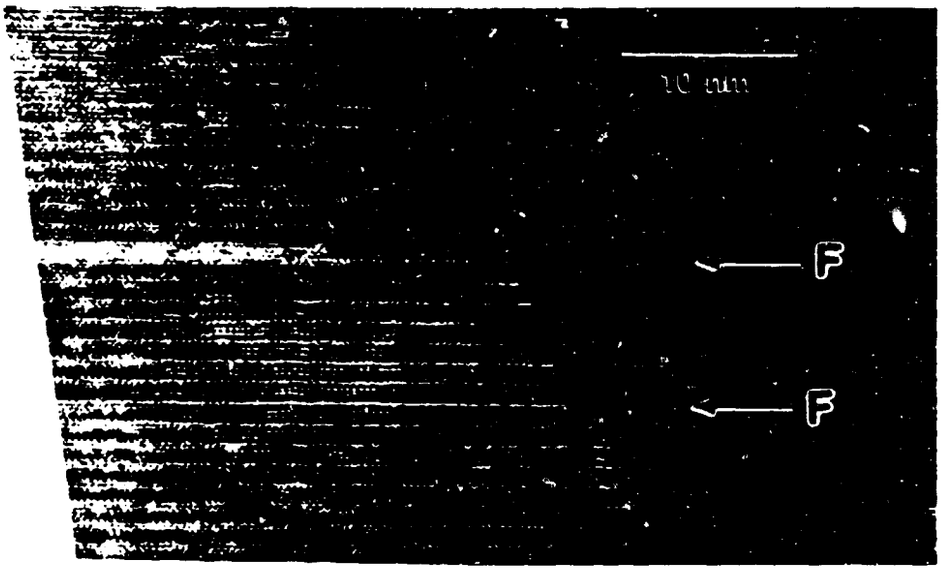

Figure 7. HREM image of 90° grain boundaries between c-pe ‹dicular and c-parallel grains in Y123.

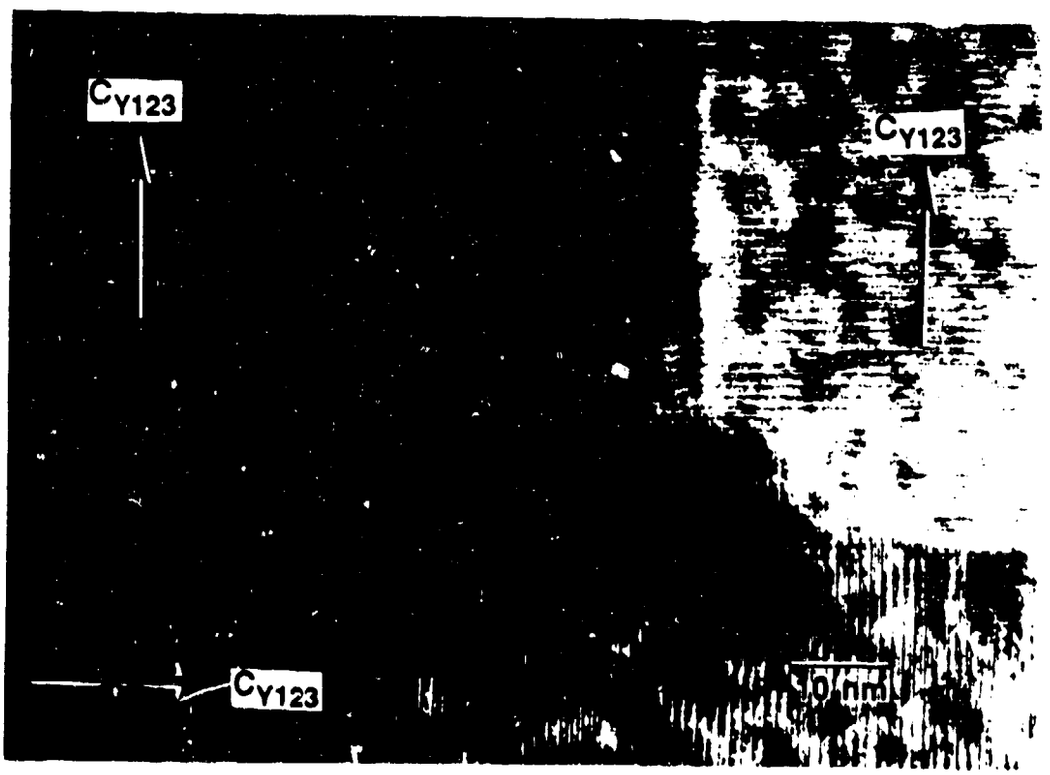

Figure 8. HREM image of faults (extra Cu-O layers labeled F) on the (001) plane of Y123.

to local deviations from stoichiometry. In fact, ordered arrangements of faults along the c-axis can produce the 247 and 248 structures, both of which have been observed in thin films [5].

Low angle boundaries are also quite common in the transition region between the inner and outer layers. An example is shown in Fig. 9. These are commonly in the (001) plane with a tilt axis of [100] or [010]. They are therefore made up of edge dislocations with a Burgers vector of [001]; such dislocations have been observed to dissociate by climb into three 1/3[001] dislocations [21]. These low angle boundaries help accommodate the small rotations that develop when the c-parallel grains nucleate on top of the c-perpendicular grains.

Laser-ablated in situ films

Many of the features found in the post-situ annealed films are also observed in the laser-ablated films. An example of a low magnification cross-sectional view of Y123 on a (001)$LaAlO_3$ substrate is shown in Fig. 10. Again there is an inner layer approximately 0.5μm thick of a c-perpendicular grain epitaxial with the substrate. Interface dislocations are observed with a periodicity of about 130Å, which is somewhat smaller than the expected 230Å periodicity needed to accommodate the 1.66% mismatch at 750°C. The inner layer also shows a high density of planar faults parallel to the (001) plane with associated partial dislocations. In the thicker regions of the film, Fig. 10 shows that c-parallel grains have nucleated. However, their morphology is different from that in the post situ annealed films where the 90° grain boundaries tend to be flat and parallel to the substrate. In the laser-ablated films (Fig. 10), the c-parallel grains tend to be wedge-shaped; they appear to nucleate at a point and thicken gradually during growth. The high resolution micrograph in Fig. 11 shows the ledges in the 90° grain boundary between the c-parallel and c-perpendicular grains that result from the thickening process.

The growth of the c-parallel grains again gives rise to a rough surface. This is shown in Fig. 12 where SEM micrographs of films of three thicknesses (0.08, 0.55, and 0.78μm) are depicted. The increasing roughness with increasing thickness is evident. The rectangular grains correspond to the two orientations of c-parallel grains. The round grains are particulates which are ejected from the target during laser ablation;

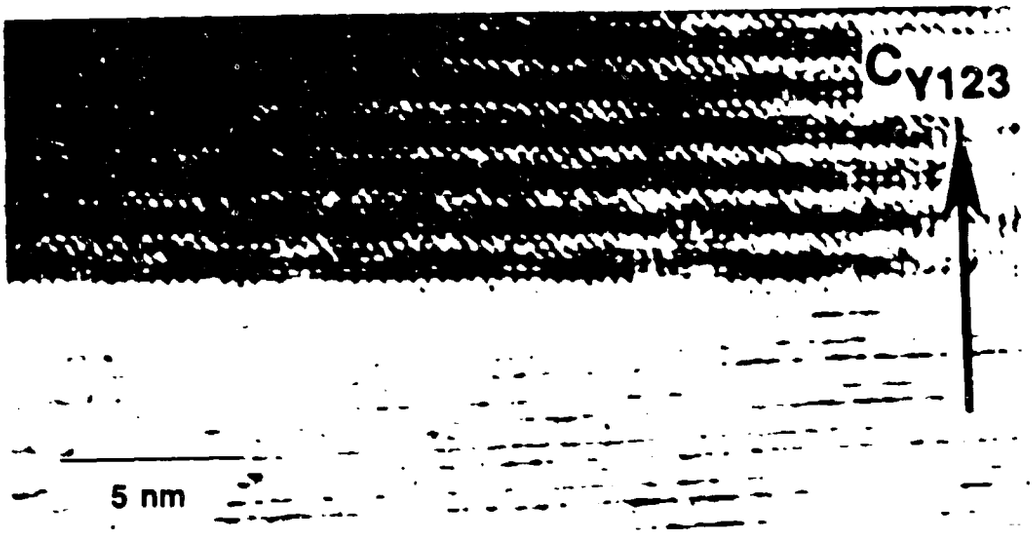

Figure 9. HREM image of a low angle grain boundary in Y123.

Figure 10. Bright-field TEM image of Y123 film grown on $LaAlO_3$. Note the interface dislocations, the defects in the Y123, the wedge-shaped c-parallel grains and the misoriented particulate grain.

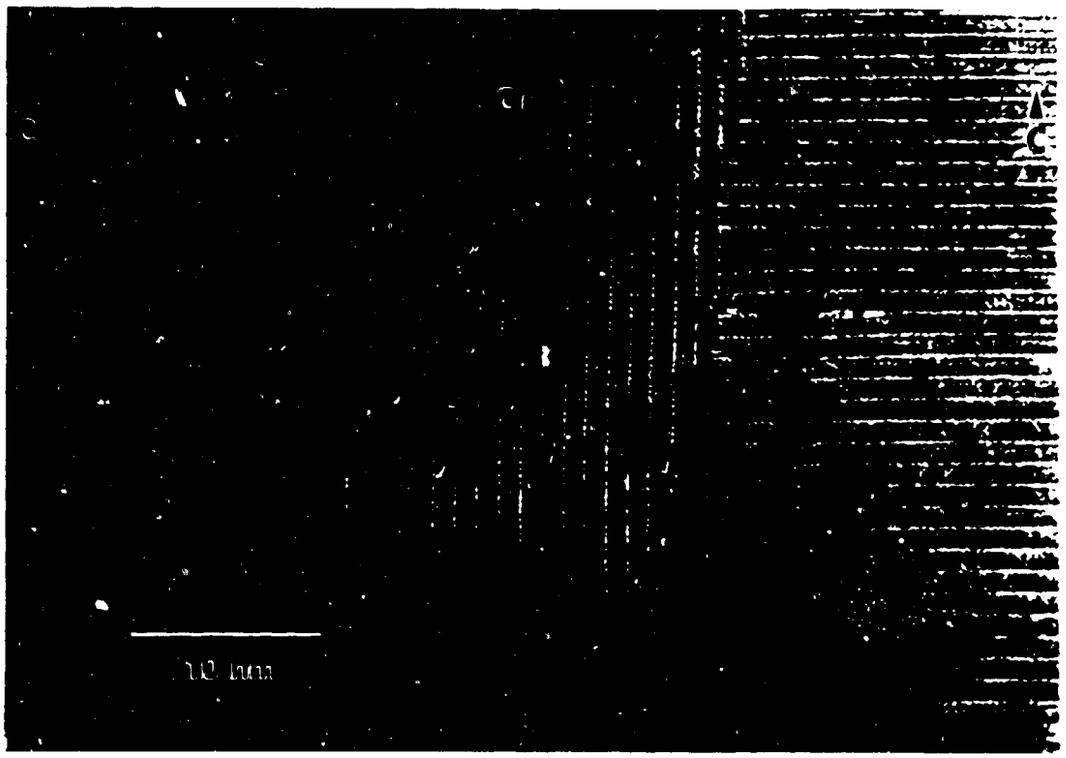

Figure 11. HREM of a c-parallel grain showing ledges in the 90° grain boundaries.

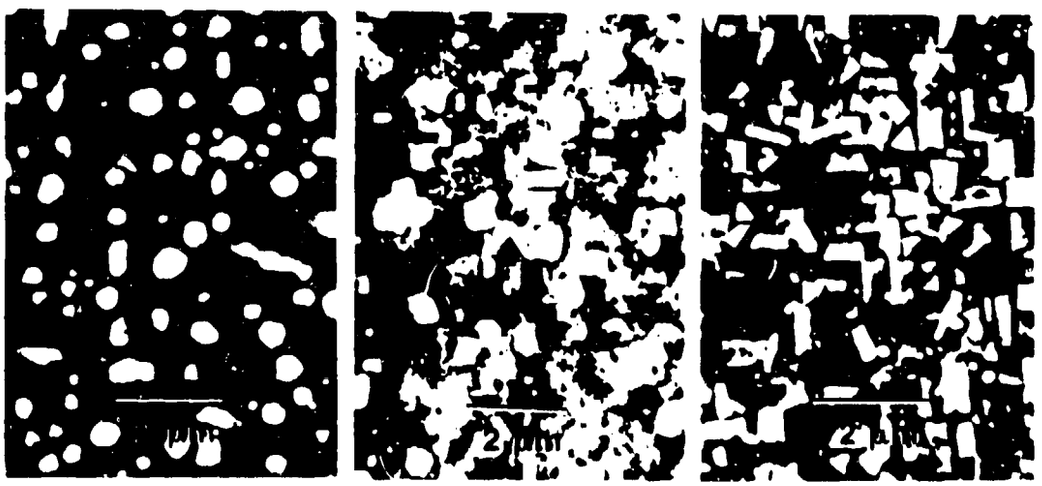

Figure 12. SEM micrographs of laser-ablated films of thickness 0.08μm (left), 0.55μm (middle) and 0.78μm (right).

they appear to be deposited in an amorphous form and then crystallize in random orientations. They are clearly deleterious to the thin film properties and they need to be eliminated by modification of the processing technology.

A high resolution electron micrograph of the interface is shown in Fig. 13. There are regions of good fit separated by regions of bad fit. The latter correspond to the misfit dislocations described earlier; however, they show more strain contrast than expected. This could be due to the phase transformations that occur in both the superconductor and substrate during cooling where the transformation strain is somehow concentrated around the misfit dislocations. There is no evidence of amorphous regions or interdiffused regions at the substrate, indicating that the correct chemistry of the deposit is established immediately and that the process is rapid enough to minimize interdiffusion.

Figure 13. HREM image of Y123/$LaAlO_3$ interface.

The question remains as to the nature of the defects responsible for flux pinning in the thin films. There is no doubt that the c-parallel grains are deleterious to the superconducting critical current both because of the introduction of current paths along the c-axis and because of the presence of 90° grain boundaries. The defects responsible for flux pinning in the inner c-perpendicular layer could be either sub-microscopic (oxygen vacancies or other point defects) or microscopic, namely the highly visible planar defects on the (001) plane with their

associated partial dislocations. The anisotropic nature of these planar defects may explain the dependence of the J_c versus field behavior on field direction noted in Fig. 1. Dislocations are known to be effective flux line pinners in conventional low T_c superconductors and may play the same role in high-T_c superconductors in spite of their small coherence length.

ACKNOWLEDGEMENTS

This research was supported by the Department of Energy, Office of Basic Energy Sciences. S. N. Basu, T. Roy, R. E. Muenchausen, M. Nastasi, and I. D. Raistrick variously provided specimens and helped with electron microscopy, as well as participating in stimulating discussions.

REFERENCES

1. J. Geerk, G. Linker, and O. Meyer, "Epitaxial Growth and Properties of YBaCuO Thin Films," Mater. Sci. Reports 4, 193-260 (1989).
2. T. E. Mitchell, D. R. Clarke, J. D. Embury, and A. R. Cooper, "Processing Ceramic Superconductors," JOM 41, 6-10 (1989).
3. M. Tomita, T. Hayashi, H. Takaoka, Y. Ishii, Y. Enomoto, and T. Murakami, "Cross-Sectional TEM Observation of $Ba_2YCu_3O_{7-x}$ Film on $SrTiO_3$," Japan. J. Appl. Phys. 27, L636-L638 (1988).
4. F. K. Legoues, "The Microstructure of $YBa_2Cu_3O_{7-x}$ Thin Films on $SrTiO_3$ Substrate," Phil. Mag. B 57, 167-177 (1988).
5. R. Ramesh, D. M. Hwang, T. Venkatesan, T. S. Ravi, L. Nazar, A. Inam, X. D. Wu, B. Dutta, G. Thomas, A. F. Marshall, and T. H. Geballe, "Direct Observation of Structural Defects in Laser-Deposited Superconducting Y-Ba-Cu-O Thin Films," Science 247, 57-59 (1989).
6. A. Mogro-Campero, L. G. Turner, E. L. Hall, M. F. Garbauskes, and N. Lewis, "Epitaxial Growth and Critical Current Density of Thin Films of $YBa_2Cu_3O_{7-x}$ on $LaAlO_3$ Substrates," Appl. Phys. Lett. 54, 2719-2721 (1989).
7. L. A. Tietz, C. B. Carter, D. K. Lathrop, S. E. Russek, R. A. Buhrman, and J. R. Michael, "Crystallography of $YBa_2Cu_3O_{6+x}$ Thin Film Interfaces," J. Mater. Res. 4, 1072-1080 (1989).
8. O. Eibl and B. Roas, "Microstructure of $YBa_2Cu_3O_{7-x}$ Thin Films Deposited by Laser Ablation," J. Mater. Res. 5, 2620-2632 (1990).
9. H. Suzuki, H. Kurosawa, K. Miyagawa, Y. Hirotsu, M. Era, T. Yamashita, H. Yamane, and T. Hirai, "Thin Film Structure of

$YBa_2Cu_3O_{7-\delta}$ on (001) MgO Substrate Studied by TEM," Japan. J. Appl. Phys. 29, L1648-L1651 (1990).
10. C. W. Nieh, L. Anthony, J. Y. Josefowicz, and F. G. Krajenbrink, "Microstructure of Epitaxial $YBa_2Cu_3O_{7-x}$ Thin Films," Appl. Phys. Lett. 56, 2138-2140 (1990).
11. T. E. Mitchell, S. N. Basu, M. Nastasi, and T. Roy, "HREM of Epitaxial $YBa_2Cu_3O_7$ Thin Films," Mater. Res. Soc. Symp. Proc. 183, 357-362 (1990).
12. C. L. Jia, B. Kabius, H. Soltner, U. Poppe, and K. Urban, "A Study of the Microstructure of Epitaxial Heterostructures of $YBa_2Cu_3O_7$ and $PrBa_2Cu_3O_7$," Physica C 167, 463-471 (1990).
13. C. B. Eom, A. F. Marshall, S. S. Laderman, R. D. Jacowitz, and T. H. Geballe, "Epitaxial and Smooth Films of a-Axis $YBa_2Cu_3O_7$," Science 249, 1549-1552 (1990).
14. T. S. Ravi, D. M. Hwang, R. Ramesh, S. W. Chan, L. Nazar, C. Y. Chen, A. Inam, and T. Venkatesan, "Grain Boundaries and Interfaces in Y-Ba-Cu-O Films Laser Deposited on Single-Crystal MgO," Phys. Rev. B42 (1990).
15. R. Ramesh, D. M. Hwang, J. B. Darner, L. Nazar, T. S. Ravi, A. Inam, B. Dutta, X. D. Wu, and T. Venkatesan, J. Mater. Res. 5, 704-716 (1990).
16. T. Roy, I. D. Raistrick, and T. E. Mitchell, "Microstructures of Y123 Films on $SrTiO_3$, $LaGaO_3$ and $LaAlO_3$," Mater. Res. Soc. Symp. Proc. 169, 699-702 (1990).
17. R. E. Muenchausen, K. M. Hubbard, S. Foltyn, R. C. Estler, N. S. Nogar, and C. Jenkins, "Effects of Beam Parameters on Excimer Laser Deposition of $YBa_2Cu_3O_{7-\delta}$," Appl. Phys. Lett. 56, 578-580 (1990).
18. E. D. Specht, C. J. Sparks, A. G. Dhere, J. Brynestad, O. B. Cavin, D. M. Kroeger, and H. A. Oye, "Effect of Oxygen Pressure on the Orthorhombic-Tetragonal Transition in the High-Temperature Superconductor $YBa_2Cu_3O_x$," Phys. Rev. B 32, 7426-7434 (1988).
19. H. M. O'Bryan, P. K. Gallagher, G. W. Barkstresser, and C. D. Brandle, "Thermal Analysis of Rare Earth Gallates and Aluminates," J. Mater. Res. 5, 183-189 (1990).
20. M. Fendorf, C. P. Burmester, L. T. Wille and R. Gronsky, "Epitaxial and Theoretical Characterization of the $YBa_2Cu_3O_7/YBa_2Cu_3O_6$ Phase Transformation," J. Less-Common Metals 164 & 165, 84-91 (1990).
21. M. F. Chisholm and D. A. Smith, "Low-Angle Tilt Grain Boundaries in $YBa_2Cu_3O_7$ Superconductors," Phil. Mag. A59, 181-197 (1989).